Stickiness in mushroom billiards

Eduardo G. Altmann*

Max Planck Institute for the Physics of Complex Systems, Nöthnitzer Strasse 38, 01187 Dresden, Germany

Adilson E. Motter

Center for Nonlinear Studies and Complex Systems Group, Theoretical Division, Los Alamos National Laboratory, MS B258, Los Alamos, NM 87545, USA and
Max Planck Institute for the Physics of Complex Systems, Nöthnitzer Strasse 38, 01187 Dresden, Germany

Holger Kantz

Max Planck Institute for the Physics of Complex Systems, Nöthnitzer Strasse 38, 01187 Dresden, Germany.

We investigate dynamical properties of chaotic trajectories in mushroom billiards. These billiards present a well-defined simple border between a single regular region and a single chaotic component. We find that the stickiness of chaotic trajectories near the border of the regular region occurs through an infinite number of marginally unstable periodic orbits. These orbits have zero measure, thus not affecting the ergodicity of the chaotic region. Notwithstanding, they govern the main dynamical properties of the system. In particular, we show that the marginally unstable periodic orbits explain the periodicity and the power-law behavior with exponent $\gamma = 2$ observed in the distribution of recurrence times.

The stickiness of chaotic trajectories in Hamiltonian systems, characterized by long tails in the recurrence time statistics, is usually associated with the presence of partial barriers to the transport in the neighborhood of hierarchies of Kolmogorov-Arnold-Moser (KAM) islands. However, as we show, these hierarchical structures are not necessary for the occurrence of stickiness. Here we study mushroom billiards (1), which are analytically solvable systems without hierarchies of KAM islands, and we show that these systems present stickiness due to the presence of one-parameter families of marginally unstable periodic orbits within the chaotic region.

I. INTRODUCTION

An important property of the dynamics in Hamiltonian systems with mixed phase space, where regions of regular and chaotic motion coexist, is the stickiness (2) of chaotic trajectories near the border of KAM islands. These chaotic trajectories experience long periods of almost regular motion, which strongly influence global properties of the system, such as transport (3) and decay of correlations (2). Even though no universal scenario exists (3),

stickiness in Hamiltonian systems is in general related to topological properties of invariant structures in the phase space (4; 5). In the widely studied case of Hamiltonian systems with hierarchies of infinitely many KAM islands, there has been an intense debate about the possible universality of the scaling exponents in the recurrence time statistics (RTS) (3; 5; 6; 7; 8). The difficulty in that case is partially due to the complexity of the invariant structures in the phase space. It is thus of substantial interest the study of Hamiltonian systems with simpler phase space, where the RTS can be studied analytically.

Recently, Bunimovich (1; 9) introduced a new family of Hamiltonian systems, the so called mushroom billiards, which have the remarkable non-generic property of having a phase space with a single KAM island and a single ergodic chaotic region. In FIG. 1, we show an example of mushroom billiard consisting of a semi-circle (*hat*) placed on top of a triangle (*foot*). In the configuration space, the border between the island and the chaotic sea consists of the orbits in the semi-circular hat of the billiard that are tangent to the circle of radius r in FIG. 1a. The regular region (KAM island) is composed of the trajectories that do not cross this circle, remaining forever in the semi-circular hat. The chaotic component consists of the complementary set of trajectories, those that cross the dashed circle and may visit the foot of the mushroom. Except for zero measure sets, which are discussed in detail in this article, all trajectories in the chaotic region indeed visit the foot of the mushroom. The stickiness close to the border of the chaotic region does not depend on the specific format of the foot as far as the foot provides a chaotic injection of the trajectories into the hat (where

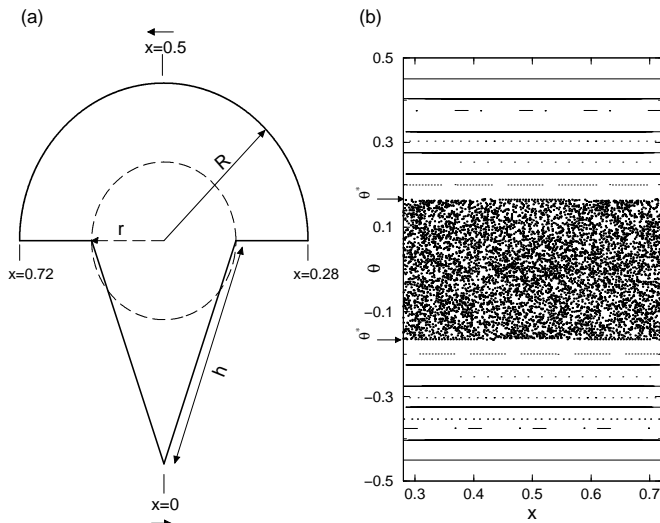*Author to whom correspondence should be sent. E-mail address: edugalt@mpipks-dresden.mpg.de

FIG. 1 A mushroom billiard with triangular foot. (a) Configuration space. (b) Phase-space representation of the semi-circular hat, where x is the normalized position and θ is the normalized reflection angle. The parameters are $r/R = 0.6125$ and $h/R = 1.5$, what implies $\theta^* = \pm 1/6$.

the stickiness occurs). The coordinates used to describe the phase space are the normalized position $x \in [0,1]$ along the boundary of the billiard and the normalized angle $\theta \in [-0.5, 0.5]$ with respect to the normal vector right after the specular reflection. With respect to these coordinates, the border between the regular and the chaotic regions for trajectories in the semi-circular hat is at $\theta^*(r/R) = \pm \sin^{-1}(r/R)$, as shown in Fig. 1b. The important control parameter is the ratio r/R and the time is counted as the number of reflections. Precise experimental realizations of billiards, e.g., in microwave cavities and atom optics (10), have generated additional motivation for the investigation of the dynamics of these billiards.

In this article, we study the properties of stickiness in mushroom billiards. Two important features are observed in the RTS: (i) periodicities in the sequence of recurrence times and (ii) a power-law distribution with scaling exponent $\gamma = 2$ in the limit of long recurrence times. Both effects are consequence of the presence of one-parameter families of marginally unstable periodic orbits (MUPOs) inside the chaotic region, which are studied here in detail. While the specific properties of the former effect are strongly dependent on the particular value of the control parameter r/R, the latter is invariant under changes of r/R.

The article is organized as follows. In Sec. II, we motivate the problem with numerical observations of stickiness in mushroom billiards. The general characterization of MUPOs in mushroom billiards is presented in Sec. III. In Sec. IV, MUPOs are used to describe the effects (i) and (ii) in the stickiness of the chaotic trajectories. A summary of the conclusions is presented in the last section.

tion.

II. NUMERICAL OBSERVATION OF STICKINESS

In this section, numerical observations of the stickiness in mushroom billiards are reported. We quantify the stickiness through the RTS, as follows. The whole foot of the billiard is chosen as the recurrence region. A typical trajectory is initialized within the recurrence region and followed for a long time. The time T the trajectory takes, after leaving the recurrence region, to return to it for the first time is recorded. Through further iterations of the same trajectory, an arbitrarily long sequence of recurrence times, distributed according to $P(T)$, can be obtained. The RTS is then defined as

$$Q(\tau) = \sum_{T=\tau}^{\infty} P(T) = \lim_{N \to \infty} \frac{N_\tau}{N} , \qquad (1)$$

where N is the total number of recurrences and N_τ is the number of recurrences with time $T \geq \tau$. For long times, in hyperbolic chaotic systems, the RTS decays exponentially (11), while in systems with stickiness, it decays roughly as a power law (2; 3),

$$Q(\tau) \propto \tau^{-\gamma},$$

where $\gamma > 1$ is the scaling exponent (see also Ref. (12)). In our numerics, we approximate Eq. (1) with a finite, statistically significant number N of recurrences.

Our main observations about the RTS in the mushroom billiard are illustrated in FIG. 2 and can be summarized as follows:

(i) The recurrence times T for which recurrences are observed appear in a very organized way: times without a single recurrence ($P(T) = 0$) are periodically interrupted by times with a high recurrence time probability. The period t_0 between successive times with positive probability ($P(T) > 0$) strongly depends on the control parameter r/R and may change over large intervals of time T. In particular, as shown in the inset of FIG. 2 for recurrence times in the interval $50 < T < 150$, this period is $t_0 = 5$ for $r/R = 0.5$ and $t_0 = 11$ for $r/R = 0.6125$. For longer recurrence times, higher periods may coexist with short periods.

(ii) The overall behavior of the RTS $Q(\tau)$ shown in FIG. 2 presents a clear power-law tail with exponent $\gamma = 2$, independently of the parameter r/R.

These observations are fully explained through the analysis of MUPOs present in the chaotic component of the billiard. The existence and properties of these orbits are discussed in the next section.
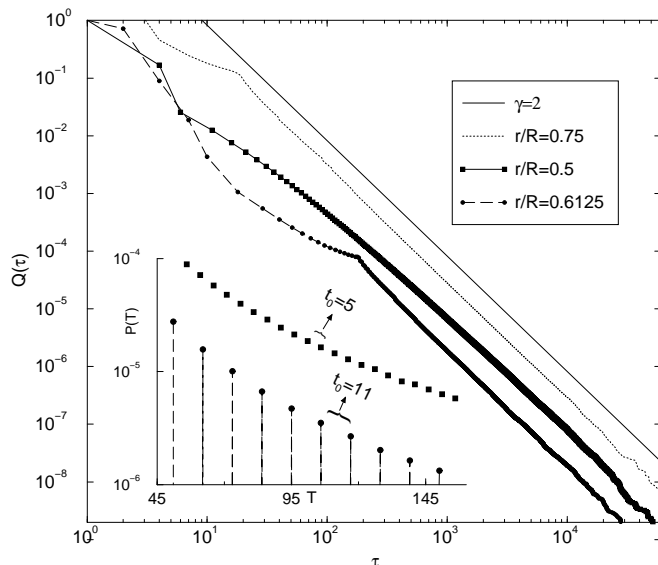
FIG. 2 RTS of the mushroom billiard for various choices of the control parameter r/R. The results are consistent with a power-law tail with exponent $\gamma = 2$. The distribution for $r/R = 0.75$ was shifted vertically upward by one decade for clarity. Inset: the distribution $P(T)$ in the interval $50 < T < 150$ for $r/R = 0.5$ ($t_0 = 5$) and $r/R = 0.6125$ ($t_0 = 11$).

III. MUPOS INSIDE THE CHAOTIC REGION

The chaotic trajectories in the mushroom billiard always visit the foot of the mushroom while the regular trajectories are confined to the hat of the billiard. The integrability of the latter trajectories is based on the conservation of the reflection angle θ for collisions in the semi-circular hat. The novel aspect shown here is that there are angle-preserving periodic orbits *inside* the chaotic region that never visit the foot of the mushroom, and they form one-parameter families of MUPOs. We use the acronym MUPO to refer specifically to marginally unstable periodic orbits belonging to this class of orbits. They have zero Lyapunov exponent and, in contrast with elliptic points, their eigenvalues are real and have modulus one. In this section, we study the stability and distribution of these MUPOs based on the analysis of an equivalent open circular billiard.

A. Open circular billiard

A convenient way to visualize the MUPOs is to consider a circular billiard of radius R, as depicted in FIG. 3a, which has the property that trajectories are considered to escape when they hit the horizontal straight-line segment of length $2r$ in the center of the billiard (hereafter referred to as the *hole*). The equivalence between the two billiards is based on the application of the image construction "trick" to the horizontal segments in the hat of the mushroom billiard and on the

independence on the shape of the foot (1). The coordinates of the circular billiard are the reflection angle $\theta \in [-0.5, 0.5]$ with respect to the normal vector and the position of collision in the circumference, given by the angle $\phi \in [-\pi, \pi]$, as indicated in FIG. 3a. The time is again measured as the number of reflections at the border of the billiard. This introduces a minor difference between the two billiards since in the mushroom billiard one counts the reflections at the horizontal segments of the hat. Nevertheless, the dynamics of the trajectories in the open circular billiard is equivalent to that of trajectories in the semi-circular hat of the mushroom billiard, where stickiness occurs and where the MUPOs are located. Geometrically, the MUPOs are the periodic orbits of the open circular billiard that cross the circle of radius r but that do not hit the hole in the center of this circle. Examples of MUPOs are shown in Figs. 3 and 5 for the parameters $r/R = 0.5$ and $r/R = 0.6125$.
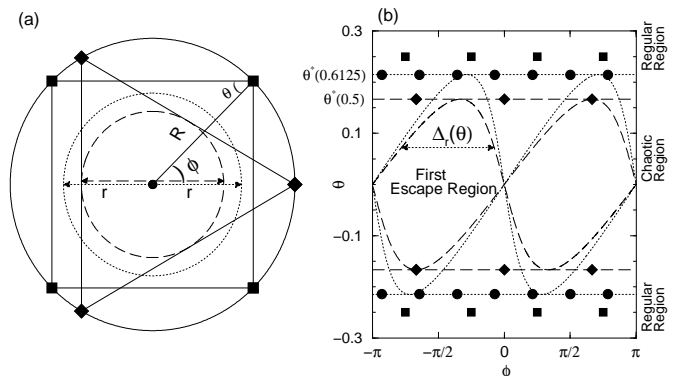

FIG. 3 (a) The open circular billiard for two different lengths of the hole: $r/R = 0.5$ and $r/R = 0.6125$. Diamonds ($\blacklozenge$) correspond to a periodic orbit ($q = 3, \eta = 1$) and squares ($\blacksquare$) to a periodic orbit ($q = 4, \eta = 1$). (b) Phase-space representation of (a). Circles ($\bullet$) correspond to a periodic orbit ($q = 7, \eta = 2$), which is studied in detail in FIG. 5, and the other symbols are the same as in (a). The four horizontal lines represent the border θ^* between the chaotic and regular regions. The first escape regions for $r/R = 0.5$ and $r/R = 0.6125$ are the areas limited by the dashed and dotted curves, respectively.

We now describe the necessary and sufficient conditions for the existence of MUPOs inside the chaotic region of the mushroom billiard. A periodic orbit in the open circular billiard is defined by two integer numbers: the period q and the rotation number η (i.e., the number of laps around the center of the circle), where q/η is an irreducible fraction and $q > 2\eta$. The invariant reflection angle θ of this orbit is given by $\theta_p(q, \eta) = \pm(q - 2\eta)/2q$.

The first necessary condition for the existence of a MUPO defined by q and η is that the corresponding trajectory crosses the circle of radius r, meaning that the trajectory would be inside the chaotic component of the original mushroom billiard. Accordingly, the reflection

angle of this orbit must satisfy

$$|\theta_p(q,\eta)| = \frac{q - 2\eta}{2q} < \frac{1}{\pi}\sin^{-1}(r/R) = |\theta^*(r/R)|. \quad (2)$$

The second necessary condition for this orbit to be a MUPO is that its trajectory does not hit the hole. In order to study this condition in the phase space of the open circular billiard, we analyze the points with reflection angle θ that hit the hole in one time step. These points define what we call the *first* escape region, whose width we denote by $\Delta_r(\theta)$ (see FIG. 3b). The trajectory does not hit the hole if all the q periodic points of the orbit are outside the first escape region. With respect to the coordinate ϕ, the distance between two neighboring periodic points is constant, namely $2\pi/q$. The second condition can thus be written as

$$\frac{2\pi}{q} > j\Delta_r(\theta_p), \quad j = \begin{cases} 1 & \text{if } q \text{ is even,} \\ 2 & \text{if } q \text{ is odd.} \end{cases} \quad (3)$$

The factor $j = 2$ for the odd-period periodic orbits comes from the 2π periodicity of the points of these orbits in opposition to the π periodicity of the escape region.

To calculate $\Delta_r(\theta)$, we have to determine the borders of the first escape region (FIG. 3b). For a given position ϕ in the circumference of radius R, the angles θ of the trajectories that first hit the hole are limited by the angles $\theta^{\pm}$ given by

$$\begin{aligned} \theta^+ &= \frac{1}{2\pi}[\phi + \tan^{-1}(\frac{R\sin(\phi)}{r + R\cos(\phi)})], \\ \theta^- &= \frac{1}{2\pi}[\frac{\pi}{2} - \phi + \tan^{-1}(\frac{R\cos(\phi) - r}{R\sin(\phi)})]. \end{aligned} \quad (4)$$

The width of the first escape region is then given by

$$\Delta_r(\theta_p) = \phi_1^{\pm} - \phi_2^{\pm}, \quad (5)$$

where $\phi_1^{\pm} > \phi_2^{\pm}$ are the two solutions of the equation $\theta^{\pm} = \theta_p$. Observe that, because of the symmetry $\theta \to -\theta$, we have $\phi_1^+ - \phi_2^+ = \phi_1^- - \phi_2^-$.

Gathering all these, we have that the conditions expressed in the Eqs. (2) and (3) are not only necessary but also sufficient for an orbit with period q and rotation number η to be a MUPO inside the chaotic region of the original mushroom billiard. These conditions can be translated in terms of the interval of the control parameter r/R for which a given periodic orbit (q, η) is a MUPO:

$$\sin[\pi\theta_p(q,\eta)] < r/R < \frac{\sin[\pi\theta_p(q,\eta)]}{\cos[\pi/(jq)]}, \quad (6)$$

with j as in Eq. (3). In Fig. 4, we show the parameters for which the orbits up to period $q = 20$ are MUPOs. An efficient procedure to find higher order MUPOs for a given parameter r/R is to take η/q as the convergents of the continuous fraction expansion of $\frac{1}{\pi}\cos^{-1}(r/R)$ and verify if they fulfill condition (6) or, equivalently, Eqs. (2) and (3). Through this procedure we have found the following MUPOs for $r/R = 0.625$: $(q, \eta) = (7, 2)$, $(698, 199)$, $(1161, 331)$, $(18341, 5229)$, $(2136146, 609013)$, and $(8526243, 2430823)$.
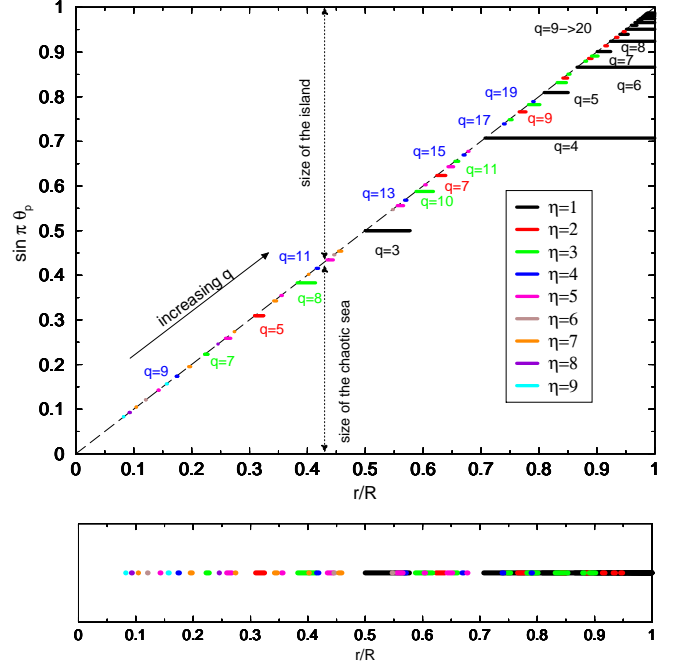

FIG. 4 (Color) Intervals of the control parameter r/R for which orbits (q, η) are MUPOs. All orbits with $q \leq 20$ are shown.

B. Stability of periodic orbits

In this section we show that the periodic orbits considered in Sec. III.A are marginally unstable, i.e., are unstable but have zero Lyapunov exponent, and that they form one-parameter families in the phase space. Consider small perturbations to one of these orbits. If the initial position ϕ is perturbed, neglecting the presence of the hole, an equivalent orbit rotated in the configuration space is always obtained (FIG. 5). When we consider the presence of the hole, some of these orbits escape and create gaps in the possible ϕ values of the periodic orbits. However, when the (strict) inequalities in Eqs. (2) and (3) are satisfied, there remain (open) intervals of ϕ values in between these gaps. These remaining intervals define a one-parameter family of MUPOs with constant θ. A small perturbation in the angle $\theta' = \theta - \varepsilon$, on the other hand, leads to an increase $\phi' - \phi = 2\varepsilon$ per time step in the distance from the original unperturbed orbit. This shows that the separation increases linearly in time and hence that these periodic orbits are indeed marginally unstable. Since the marginal stability does not depend on the discretization of time, the statistical properties of the recurrence time discussed in this article remain valid for continuous time dynamics.

Typically, a MUPO perturbed with respect to (θ, ϕ) is a quasi-periodic orbit in the circular billiard, which, without the hole, would pass arbitrarily close to all values of ϕ. Because of this ergodicity with respect to the coordinate ϕ, the corresponding perturbed trajectory eventually enters the first escape region and hits the hole, as
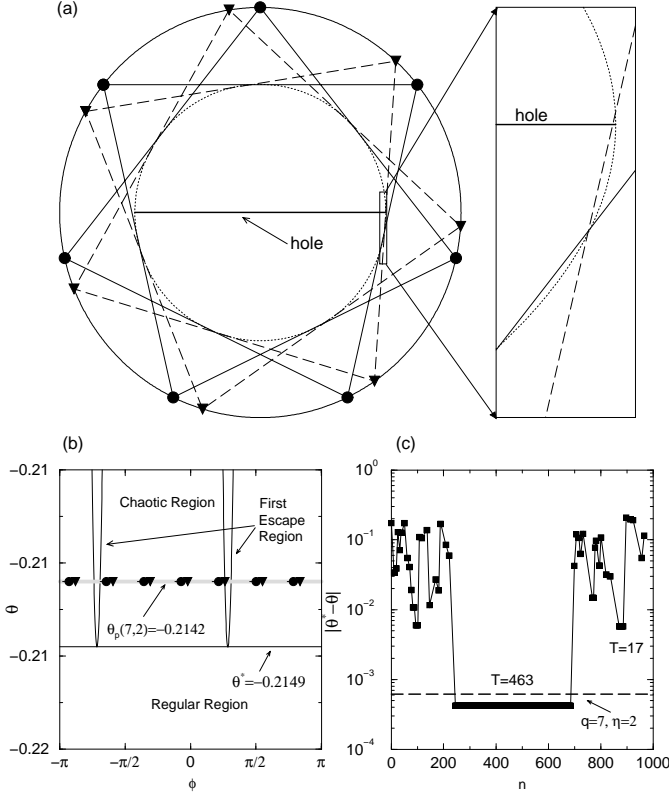
FIG. 5 Detailed analysis of orbits $(q = 7, \eta = 2)$ for $r/R = 0.6125$. (a) Configuration space, where two orbits $(q = 7, \eta = 2)$ that cross the circle with radius r are shown. The orbit represented by circles ($\bullet$) does not hit the hole, while the orbit represented by triangles ($\blacktriangledown$) hits the hole on the right-hand side (see amplification). (b) Phase-space representation of the orbits in (a), where it is shown that they are respectively outside and inside the first escape region. A small perturbation in the reflection angle θ of the first orbit leads to a continuous rotation of the orbit in (a) [horizontal drift in (b)] until the trajectory hits the hole [enters the first escape region in (b)]. (c) Time evolution of the distance from the regular region to a chaotic trajectory that approaches the family of MUPOs $(q = 7, \eta = 2)$ in the original mushroom billiard. Events with recurrence time $T = 463$ and $T = 17$ are highlighted. The events with large recurrence times are associated with approaches to the MUPOs.

illustrated in FIG. 5. The distance from the unperturbed MUPO grows linearly in time. However, the distance ε from the corresponding *family* of MUPOs remain constant until the perturbed trajectory hits the hole and escapes (FIG. 5c).

C. Distribution of families of MUPOs

We now use the information about the first escape region, Eq. (5), to study how the families of MUPOs are distributed inside the chaotic region of the mushroom billiard. The MUPOs are the only orbits in the mushroom's hat that cross the circle of radius r but never

visit the foot of the mushroom (Fig. 1a). Equivalently, in the open circular billiard, these are the orbits that cut the circle of radius r but never escape (Fig. 3a). In FIG. 6, we show the phase space of the open circular billiard for trajectories $|\theta| < |\theta^*|$, associated with the chaotic region of the mushroom billiard, and the Nth escape region, defined by the $(N-1)$th pre-image of the first escape region shown in FIG. 3b. We note that the larger the period of the orbit the closer it may be to the border θ^*. For example, for the control parameter $r/R = 0.6125$ considered in FIG. 6, the border is at $\theta^* = 0.2149010...$ and the orbits $(q = 7, \eta = 2)$, $(q = 235, \eta = 67)$ and $(q = 698, \eta = 199)$ highlighted in the figure are at $\theta_p = 0.2143857...$, $\theta_p = 0.2148936...$ and $\theta_p = 0.2148997...$, respectively. The widths of the escape regions go to zero when the border is approached. In Fig. 6, the MUPOs correspond to the points that do not belong to any of the nth escape regions, for all $n < N$ in the limit of $N \to \infty$. That is, taking the limit $N \to \infty$ in FIG. 6, all the points outside the escape regions belong to MUPOs. Note that a complex distribution of families of MUPOs may exist near the border of the island.
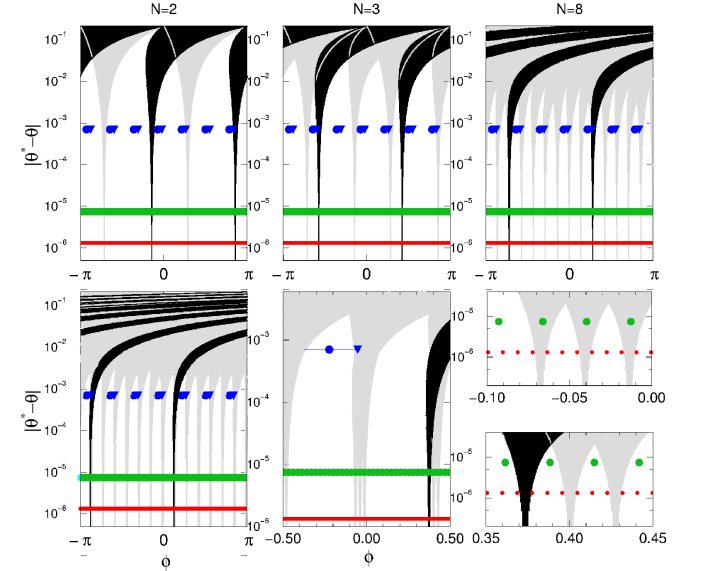

FIG. 6 (Color online) Escape regions in the the phase space of the open circular billiard for $r/R = 0.6125$. In each panel, the Nth escape region is shown in black and the nth escape regions for all $n < N$ are shown in gray. In the first row, we show the cases $N = 2$, $N = 3$, and $N = 8$, while in the second row we show the case $N = 20$ and successive amplifications for this case. Different symbols correspond to the different orbits $(q = 7, \eta = 2)$, $(q = 235, \eta = 67)$, and $(q = 698, \eta = 199)$, from top to bottom, respectively. The figures at the bottom right show that only the first and the last of these orbits are MUPOs.

IV. MUPOS AND STICKINESS

In this section, we show how the MUPOs characterized in Sec. III affect the stickiness of chaotic trajectories in the mushroom billiard and explain the numerical results reported in Sec. II. Qualitatively, the stickiness of chaotic trajectories in mushroom billiards can be described as follows. A chaotic trajectory bounces in the foot of the mushroom until it enters the semi-circular hat. Depending on the reflection angle θ, which is conserved for collisions in the hat, the trajectory may be close to a MUPO. In this case, it remains close to the family of this MUPO a long time before falling again into the foot of the billiard (see FIG. 5c). In the phase space, these events with large recurrence time are observed as a continuous rotation of the trajectory around the regular island, at a fixed distance from the island, until it enters the first escape region.

We now show how the MUPOs explain quantitatively the two effects observed in the RTS and anticipated in Sec. II:

(i) **Regularity in the distribution** $P(T)$. When a chaotic trajectory visits the hat of the billiard, the approach to as well as the escape from the neighborhood of a family of MUPOs takes place in a single time step, as illustrated in FIG. 5c by a sharp transition before and after the interval of minimum distance to the island. Due to the injection of trajectories from the foot of the mushroom billiard, the approach to the MUPOs (that requires an angle θ close to θ_p) can only occur close to some of the q periodic points of the MUPO. Actually, it happens always near the same position in the mushroom's hat, right above the intersection point between the boundary of the foot and the bottom part of the hat (i.e., one of the two horizontal lines). Similarly, the escape occurs always when the trajectory is close to the point of the MUPO that lies in the bottom part of the mushroom's hat. Due to these constraints, the intervals of time a chaotic trajectory that approaches a family of MUPOs spends away from the mushroom's foot form a sequence that can be written as $T_i = a - 1 + (q + 2\eta)i$, where $i \in \mathbb{N}$ and a is the time between the first collision in the semi-circular hat and the collision in the bottom part of the hat (close to the hole). The period t_0 between successive recurrence times with positive probability, reported in Sec. II, is thus related to the period q and the rotation number η of the MUPO inside the chaotic region according to

$$t_0 = q + 2\eta . \tag{7}$$

The factor 2η comes from the fact that, in contrast with the open circular billiard, in the mushroom billiard one counts the collisions in the bottom of the hat. In FIG. 3 we show that for $r/R = 0.5$ the orbit ($q = 3, \eta = 1$) is exactly in the border between the regular island and the chaotic region. Through Eq. (7) we obtain $t_0 = 5$, explaining the numerical observation. Analogously for the parameter $r/R = 0.6125$, in FIG. 5 we see the orbit ($q = 7, \eta = 2$) that implies $t_0 = 11$, exactly as ob-

served numerically. Higher-order periodicities are associated with the existence of additional families of MUPOs in the chaotic sea, as shown in Sec. III.C.

(ii) $\gamma = 2$ **in the tail of the RTS.** In the stability considerations described in Sec. III.B, we noticed that when we perturb a MUPO, the distance from the unperturbed orbit increases linearly along ϕ and remains constant with respect to the reflection angle θ. These properties of the MUPOs in mushroom billiards are equivalent to those observed for MUPOs present in the much simpler case of billiards with parallel walls. In the latter case, the MUPOs are generated by trajectories bouncing perpendicularly between parallel walls. Billiards with parallel walls, such as the Sinai billiard and stadium billiard, have been studied extensively (13; 14; 15; 16). It has been shown that the existence of a one-parameter family of MUPOs due to parallel walls leads to an exponent $\gamma = 2$ in the power-law decay of the RTS (14; 15; 17). Each family of MUPOs in the mushroom billiards is equivalent to a family of MUPOs generated by the presence of parallel walls. The same is true for the family of periodic or quasi-periodic marginally unstable orbits always present at the border between the regular and chaotic region of the mushroom billiard. In the mushroom billiard, more than one family of marginally unstable orbits may exist. Since each of them leads to the same asymptotic exponent $\gamma = 2$, irrespective of the control parameter r/R, the overall RTS will also have scaling exponent $\gamma = 2$. A similar argument can be used to show that the same exponent governs the RTS of honey mushrooms (1), which are systems composed by a finite number of mushroom billiards.

V. CONCLUSIONS

Mushroom billiards (1) provide an example of nontrivial Hamiltonian systems with a relatively simple phase space. In contrast with previously considered Hamiltonian systems, which have a hierarchy of infinitely many regular islands, the mushroom billiards considered here have a single island. We have shown that, in spite of the simplicity of the regular region, the chaotic component of the mushroom billiards contains a complex distribution of marginally unstable periodic orbits (MUPOs). These orbits have zero measure and do not affect the ergodicity of the system. Nevertheless, the MUPOs are crucial for the understanding of important dynamical properties of the system, as shown here through the analysis of the recurrence time statistics. In particular, we have shown that these MUPOs lead to an exponent $\gamma = 2$ for the asymptotic power-law decay of the recurrence time statistics. This result leads to the interesting question of whether this scaling exponent is universal within the class of Hamiltonian systems with finite number of regular islands (17) which, in turn, may provide new insight into the problem of universality in Hamiltonian system in general.

References

[1] L. A. Bunimovich, Chaos **11**, 802 (2001).

[2] C. F. F. Karney, Physica D **8**, 360 (1983).

[3] G. M. Zaslavsky, Phys. Rep. **371**, 461 (2002).

[4] G. M. Zaslavsky, Physica D **168-169**, 292 (2002).

[5] M. Weiss, L. Hufnagel, and R. Ketzmerick, Phys. Rev. E **67**, 046209 (2003).

[6] J. D. Meiss and E. Ott, Phys. Rev. Lett. **55**, 2741 (1985).

[7] B. V. Chirikov and D. L. Shepelyansky, Phys. Rev. Lett. **82**, 528 (1999).

[8] P. Grassberger and H. Kantz, Phys. Lett. A **113**, 167 (1985).

[9] L. Bunimovich, Chaos **13**, 903 (2003).

[10] See, for example: H.-J. Stöckmann, *Quantum Chaos: An Introduction,* (Cambridge University Press, Cambridge, 1999); A. Richter, in: *Emerging Applications of Number Theory*, The IMA Volumes in Mathematics and its Applications, Vol. 109, edited by D. A. Hejhal, J. Friedman, M. C. Gutzwiller, and A. M. Odlyzko, p. 479 (Springer, New York, 1999); N. Friedman, A. Kaplan, D. Carasso, and N. Davidson, Phys. Rev. Lett. **86**, 1518 (2001).

[11] E. G. Altmann, E. C. da Silva, and I. L. Caldas, Chaos **14**, 975 (2004).

[12] A. E. Motter, A. P. S. de Moura, C. Grebogi, and H. Kantz, Phys. Rev. E **71**, 036215 (2005).

[13] L. A. Bunimovich, Comm. Math. Phys. **65**, 295 (1979); L. A. Bunimovich and Y. Sinai, *ibid.* **78**, 479 (1980).

[14] P. Gaspard and J. R. Dorfman, Phys. Rev. E **52**, 3525 (1995).

[15] D. N. Armstead, B. R. Hunt, and E. Ott, Physica D **193**, 96 (2004).

[16] F. Vivaldi, G. Casati, and I. Guarneri, Phys. Rev. Lett. **51**, 727 (1983).

[17] E. G. Altmann, A. E. Motter, and H. Kantz (in preparation).